

Mitigation of Blast Effects on Existing Structures in Austere Environments

By
Andrew J. Maxa

B.S. Civil Engineering,
United States Military Academy 2004

Submitted to the Department of Civil and Environmental Engineering in partial fulfillment of the requirements for the degree of

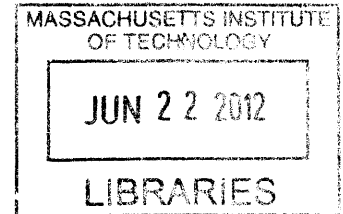
MASTER OF SCIENCE

In Civil and Environmental Engineering at the
MASSACHUSETTS INSTITUTE OF TECHNOLOGY

June 2012

© 2012 Andrew J. Maxa
All Rights Reserved

ARCHIVES



The author hereby grants to MIT permission to reproduce and to distribute publicly paper and electronic copies of this thesis document in whole or in part in any medium now known or hereafter created.

Signature of Author: _____

Andrew J. Maxa
Department of Civil and Environmental Engineering
May 15, 2012

Certified by _____

Jerome J. Connor
Professor of Civil and Environmental Engineering
Thesis Supervisor

Accepted by: _____

Heidi M. Nepf
Chair, Departmental Committee for Graduate Students

Mitigation of Blast Effects on Existing Structures in Austere Environments

By
Andrew J. Maxa

Submitted to the Department of Civil and Environmental Engineering on May 15, 2012 in partial fulfillment of the requirements for the Degree of Master of Science in Civil and Environmental Engineering.

ABSTRACT

Military commanders in austere environments often face challenges in setting up headquarters buildings that offer protected areas for sensitive equipment. One solution to this problem is simply to build a structure that can be used for this purpose. This method can prove to be difficult in that it could either require large amounts of prefabricated concrete, heavy earthmoving equipment, or a significant effort in digging by hand. Clearly, all of these options are unsuitable for constructing a headquarters building that would be occupied for a short time or if the resources required were unavailable. Another solution to this problem is to simply occupy an existing structure. This method is extremely favorable with respect to resources required; with the major drawback being that at times existing structures may offer limited protection from hostile forces. Since the US Army often has overwhelming firepower when compared to contemporary threats, many times hostile forces will resort to suicide or remotely detonated explosive devices when attempting to destroy or damage structures of this type. In order to determine the feasibility of mitigating this threat, this paper will explore the effects of various explosive devices on model building types that may be found in austere environments, and explore the effects of possible reinforcement schemes in mitigating blast threats to these structures.

Thesis Supervisor: Jerome J. Connor
Title: Professor of Civil and Environmental Engineering

Acknowledgements

To my parents, Ray and Denise, for their unending support and encouragement in all things,

To Professor Connor for making MIT such a great experience,

To my son James for always ensuring I was awake in the morning,

And to my wife Naira, for never allowing me to get complacent,

Thank you.

Table of Contents

List of Figures.....	6
List of Tables.....	7
1 Introduction.....	8
2 Method.....	10
3 Risk Assessment.....	11
4 Blast Modeling.....	15
4.1 General Characteristics.....	15
4.2 TNT Equivalence.....	16
4.3 Pressure Calculation.....	17
4.4 Structural Response to Blast Loadings.....	21
4.5 Blast X.....	22
4.5.1 Inputs.....	23
4.5.2 Calculations.....	24
4.5.3 Outputs.....	26
5 Building Models.....	27
5.1 Model with Open Doors and Windows.....	27
5.2 Model with Open Doors and Closed Windows.....	28
5.3 Model with Closed Doors and Windows.....	29
5.4 Model Failure Criteria.....	30
5.5 Model Limitations.....	30
6 Initial Simulations.....	31
6.1 Calibration Simulation.....	31
6.2 Unreinforced Simulations.....	34
6.2.1 Model with Closed Doors and Windows.....	34

6.2.2	Model with Open Doors and Closed Windows.....	37
6.2.3	Model with Open Doors and Windows.....	38
6.2.4	Model Failure Comparison.....	40
7	Carbon Reinforced Polymer.....	41
8	Reinforced Simulations	43
8.1	Reinforced Building Calibration Simulations.....	43
8.2	Reinforced Building Simulations.....	46
8.2.1	Model with Closed Doors and Windows.....	46
8.2.2	Model with Open Doors and Closed Windows.....	46
8.2.3	Model with Open Doors and Windows.....	46
9	Results Comparison.....	48
10	Conclusions.....	50
	References.....	52

List of Figures

Figure 3.1: Khobar Towers Complex.....	11
Figure 3.2: Khobar Towers BLDG 131 Damage.....	12
Figure 3.3: Explosive Damage Thresholds.....	13
Figure 4.1: Typical Incident Overpressures at Given Standoff Distances.....	15
Figure 4.2: Explosive Characteristics.....	16
Figure 4.3: Typical Blast Incident Pressure Graph.....	17
Figure 4.4: Expected Overpressures from Calculated Z Values.....	19
Figure 4.5: Reflected Pressure Coefficients.....	20
Figure 4.6: Typical Impulse Waveform	21
Figure 4.7: Structural Response Regions.....	22
Figure 4.8: Example Blast X Input.....	24
Figure 4.9: Example Calculated Blast Waveform.....	25
Figure 4.10: Blast X Validation Graph.....	26
Figure 4.11: Blast X Input Example.....	26
Figure 5.1: SAP 2000 Building Model with Doors and Windows.....	28
Figure 5.2: SAP 2000 Building Model with Door Only.....	29
Figure 5.3: SAP 2000 Building Model with no Doors or Windows.....	29
Figure 6.1: Concrete Blast Test Setup.....	31
Figure 6.2: Concrete Panel SAP 2000 Model.....	32
Figure 6.3: Incident Blast Waveform.....	32
Figure 6.4: Blast Deflection Measurement Device.....	33
Figure 6.5: Comparison of Deflected Concrete Shapes.....	33
Figure 6.6: Deflected Shape of Building without Door or Windows.....	35
Figure 6.7: Flexural Loading of Building without Door or Windows.....	36
Figure 6.8: Shear Loading of Building without Door or Windows.....	36
Figure 6.9: Deflected Shape of Building with Door but no Windows.....	37
Figure 6.10: Flexural Loading of Building with Door but no Windows.....	37
Figure 6.11: Shear Loading of Building with Door but no Windows.....	38
Figure 6.12: Deflected Shape of Building with Door and Windows.....	39
Figure 6.13: Flexural Loading of Building with Door and Windows.....	39
Figure 6.14: Shear Loading of Building with Door and Windows.....	40
Figure 8.1: CFRP Test Setup.....	43
Figure 8.2: CFRP Test Simulation Model.....	44
Figure 8.3: CFRP Test Simulation Deflected Profiles.....	45

List of Tables

Table 3.1: Considered Blast Loads.....	13
Table 4.1: Scaled Distances for considered Loads	19
Table 9.1: Building Maximum Loading Densities.....	48

1 Introduction

As typical engagements for the US Army evolve from high intensity conflict with the armies of enemy nations into those more focused on peacekeeping, its need for structures to occupy while in the field is also changing. Previously, the largest threat to our forces was hostile action from easily identifiable enemy forces, a problem that could be addressed through the application of the superior equipment and training that the US Army possesses. As the Army's role has transitioned to peacekeeping, and into building the capability of host nation police and armed forces, the threats to which it is exposed have changed as well. Threats now primarily come from small groups or individual actors who lack the capability to wage open warfare, and therefore resort to blending into the local population in order to negate the Army's obvious advantages. This also means that their preferred method of engaging US forces has changed to include methods of attack that are not easily countered by superior weaponry and training. This dynamic has shifted the primary threats the US Army faces toward those involving suicide attacks and remotely detonated explosives.

Addressing these threats clearly requires both passive and active measures. Active measures primarily consist of identifying a threat prior to an attack and actions taken after an attack, and are beyond the scope of this paper. Passive measures consist of protecting the force from the effects of attacks. As the contemporary operating environments in Iraq and Afghanistan clearly show, the currently favored method of protecting the force consists of identifying an area for an American base and ringing it with concrete walls. Easily identified examples of this are the previous Victory Base Complex at Baghdad Airport in Iraq and the current Bagram and Kandahar Airfields in Afghanistan.

As the level of US involvement in international operations decreases, the current method identified above may become less feasible. Smaller units operating in smaller areas, or units that are required to move regularly, may not have the resources required to simply place large amounts of prefabricated

concrete around a perimeter. The same resource limitations may apply to other methods currently employed, such as creating earthen walls using heavy engineering equipment, or simply hand digging fortifications.

One solution to this problem is simply to occupy structures that currently exist on the ground at convenient locations. Existing structures can be made of any type of material, but usually are some combination of low strength concrete, brick, or concrete masonry unit construction. Since the level of protection offered by these structures will usually be less than is desirable, particularly against blast loadings, steps must be taken in order to make them acceptable for use.

This paper will examine the effects of various blast loadings on simple buildings that may be found in a country where limited military operations may take place. The effects of various sizes and types of explosives will be examined, along with the effect of standoff distance on the results. Finally a typical reinforcing scheme will be applied to each building type to attempt to determine its effectiveness at reducing the effects of each blast.

2 Method

In order to determine the effects of blast loadings on buildings, the first step is to determine the blast loadings themselves. Multiple variables will alter the effects of the blast on a given structure, including the distance from the building, size and composition of explosive, and shape of the explosive. Since each situation is unique, multiple scenarios ranging from mild blasts at relatively close distances to heavier blasts further from to the structure are considered.

After the blast loadings are chosen, the pressure effects of the blasts on a given structure must be determined. In this paper, the program Blast X, developed by the Engineering Research and Development Center of the US Army Corps of Engineers, is used to do these calculations. The program considers both shockwave and gas effects in its calculations and has multiple input options that can account for all of the variations mentioned above. The program outputs the pressure incident on a designated target point. Enough target points are designated that an accurate pressure distribution across the building can be determined.

Finally, the pressure effect calculated by Blast X is applied to finite element models of various buildings. Each building considered is modeled in SAP 2000, using material definitions appropriate for the building being modeled. The dimensions are held constant between the buildings in order to have a basis for performance comparison. After initial performance measures are calculated, a reinforcement scheme is considered to be added to each building, and new results are calculated. All calculations are done using nonlinear modal analysis.

After the simulations are complete, a comparison of results, limitations of the data, and several conclusions are discussed.

3 Risk Assessment

The determination of reasonable loads is the first step when designing a structural system, and the reinforcement of existing structures for blast resistance is similar in this regard. For conventional structures, loadings are specified by a code, and then generally combined into a maximum load combination that leads to member and overall building design. In the blast retrofit process, the building has already been designed, and the engineer must first determine the size of the blast loading likely to be applied to the building. An engineer would need to consider the strength of the building, the amount of standoff possible, and the vehicular or foot accessibility to the area around the building, among other factors, when determining the risk to a particular building.

Using the Khobar Towers bombing as an example, terrorist actors were able obtain vehicular access to the area immediately adjacent to an occupied building, and used that access to devastating effect.

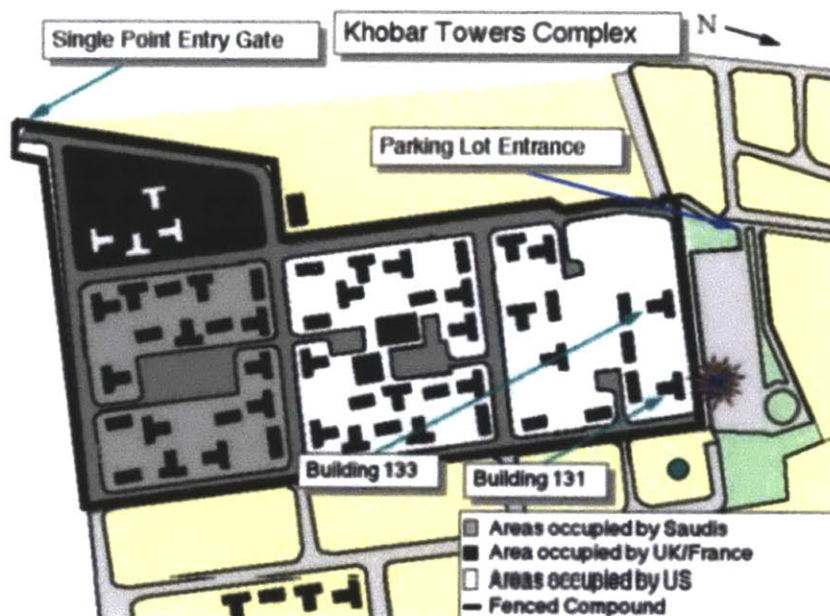


Figure 3.1: Khobar Towers Complex (Source: globalsecurity.org)

The perpetrators parked a sewage tanker truck containing the equivalent of roughly 5000 pounds of TNT about 80 feet from building 131 at the Khobar Towers complex, as shown on the diagram above. The resulting explosion killed 19 American service members and wounded approximately five hundred

others. The explosion devastated the building, shearing one face of the building off completely, as shown in the picture below (Grant).



Figure 3.2: Khobar Towers BLDG 131 Damage (Source: DefenseImagery.mil)

A force protection assessment had recently been completed prior to the detonation of the bomb, but it primarily focused on threats from bombs detonated from the inside of the compound, and on the threat from injuries caused by flying glass. Several other measures were taken to deter threats, such as placing jersey barriers outside the fence perimeter and topping the fence with concertina. However, since the parking lot used by the terrorists was often used by the Saudi population visiting a local park, the Saudi authorities would not allow the Americans to expand their perimeter, or to close off the parking lot. In hindsight a simple measure would have been to simply not inhabit the buildings that were dangerously close to the perimeter, but the Khobar Towers attack was the first large scale truck bombing that had happened in the region, and the possibility of an attack of its magnitude was not considered likely (Grant).

Using the Khobar Towers attack as a lesson, the identification of a particular site's possible avenues of approach and their associated threat levels is clearly a critical task. For the purposes of this paper, specific information on site layout and building composition are not used, simply because the

conclusions reached are meant to be broadly applicable, not limited to a particular site. Instead, multiple different explosive loads and distances are considered. The figure below is from FEMA's Risk Management Handbook, chapter 4 (FEMA Handbook), and shows reasonable thresholds for expected damage based on explosive yield and standoff distance.

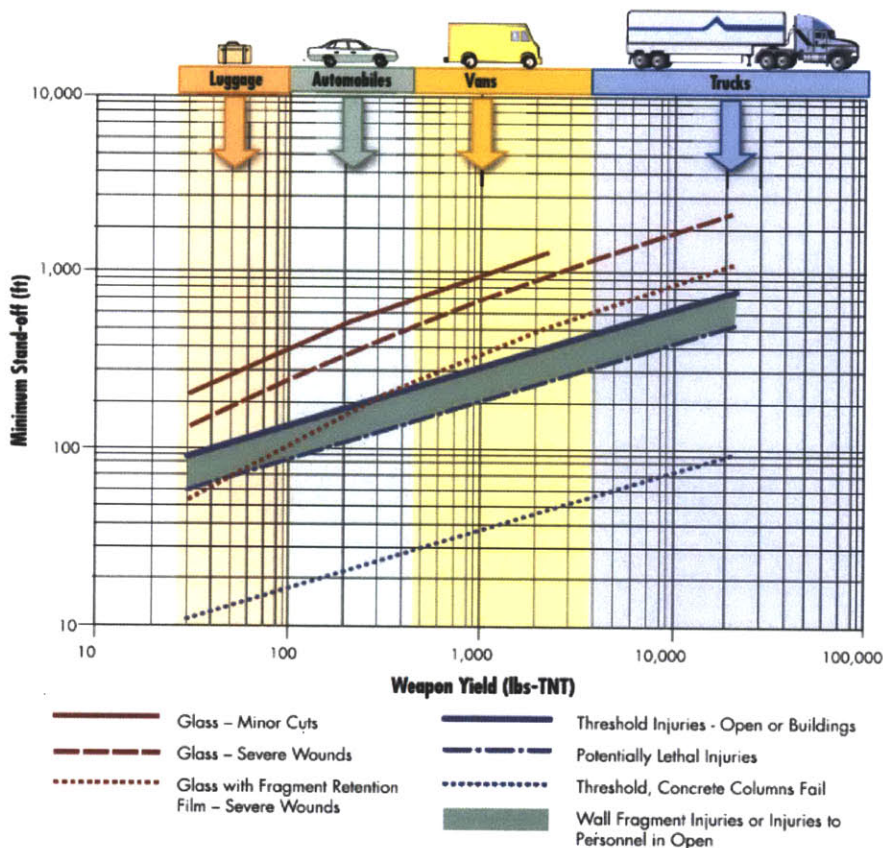


Figure 3.3: Explosive damage thresholds (Source: FEMA Handbook)

Since in this paper a specific site layout is not considered, it seems reasonable to consider a range of options, such as those shown in the figure above, in order to determine in which instances certain building types or reinforcement schemes would provide sufficient force protection.

Clearly the easiest way to transport a small bomb would be to simply carry it in a suitcase and place it on the ground next to a wall. Alternately a person wearing a suicide vest could probably get relatively close to a sensitive area before detonating a vest. As the size of the bomb increases, the size of the vehicle required to carry it would also increase. Clearly vehicles attempting to approach a sensitive building

would be increasingly suspicious as the size of the vehicle increased. A tanker truck being about 100 feet from a target building, as was the case in the Khobar Towers example, is a realistic worst case, particularly with the improved force protection measures the US currently uses. The figure below shows a list of blast loadings that will be considered in this paper.

Table 3.1: Considered Blast Loads

Source	Explosive Yield, lbs TNT	Standoff Distance, feet
Man Portable	5	5
	50	10
	50	20
Sedan	300	25
	300	50
Van	1000	40
	1000	160
Truck	5000	40
	5000	200
	10000	400

These load cases are not meant to be a complete list. The cases are meant to be a representative grouping of cases from which the effectiveness of different buildings and reinforcement schemes can be determined. In order to determine likely standoff distances at a particular site for given sources carrying given yields, a study of that particular site would need to be undertaken.

4 Blast Modeling

After deciding on the explosive compositions and standoff distances to be modeled, the next step was to determine the loadings that each blast would place on each structure.

4.1 General Characteristics

In general, a blast wave is formed by a heat producing chemical reaction. For example, when a spark and pressure are applied to a block of C4, the relatively stable solid is quickly converted into a very hot, very dense gas. Because the relative heat and density of the newly formed gas are much higher than those in the surrounding atmosphere, the gas expands at a rapid rate, creating a shockwave that travels spherically away from the center of the blast. The blast wave dissipates as it travels away from the center of the blast, until it strikes a surface and is reflected, or until it reaches an equilibrium condition with the surrounding air. If the shockwave strikes a structure, the reflected wave pressure is the pressure that is applied to the face of a structure. The table from the FEMA Handbook below shows general expected incident overpressure values for given net explosive weights at given standoff distances. Methods for determining more exact values for these numbers are discussed below.

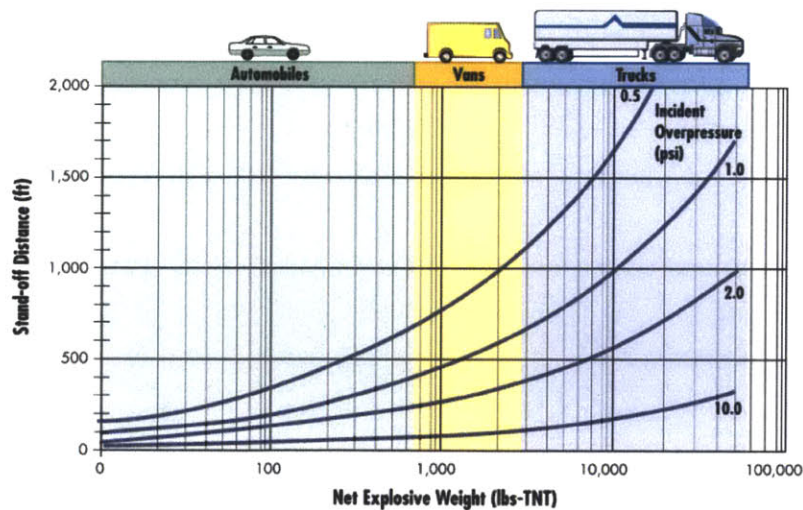


Figure 4.1: Typical Overpressures at Given Standoff Distances (Source: FEMA Handbook)

4.2 TNT Equivalence

Before calculating the effects of a blast, the explosive must first be converted to an equivalent weight in TNT by multiplying the weight of a given explosive by its RE factor. Figure 4.2 below is a partial list of RE factors for explosives generally in use by the military and is taken from US Army Field Manual 5-25. In general, explosives with a higher RE factor explode with a higher detonation velocity and are more suited to be used in smaller amounts for cutting operations. Conversely, materials with lower RE factors are better utilized in large amounts and the resulting explosions are better for pushing. For example C4 is useful for steel and timber cutting, and if used for cratering would possibly only blow a small hole in the ground along the path of least resistance to the open air, which would allow the expanding gas to quickly vent into the air and reach equilibrium. If dynamite was used to cut timber or steel it would probably simply push the material meant for cutting away from the detonation source. However, when used to create a crater, it explodes more slowly and is therefore more suitable for pushing a large amount of soil away from the detonation source and forming a crater.

Name	Principal use	Smallest cap * required for detonation	Approx. velocity of detonation (meter/sec) (feet/sec)	Relative effectiveness as external charge (TNT 1.00)	Intensity of poisonous fumes	Water resistance
TNT	Main charge, booster charge, cutting and breaching charge, general and military use in forward areas	Special blasting cap	6,900 mps 23,000 fps	1.00	Dangerous	Excellent
Tetrytol			7,000 mps 23,000 fps	1.20	Dangerous	Excellent
Composition C 3			7,825 mps 26,018 fps	1.34	Dangerous	Good
Composition C 4			8,040 mps 26,379 fps	1.34	Slight	Excellent
Ammonium Nitrate	Cratering and ditching		3,400 mps 11,000 fps	0.42	Dangerous	Poor
Military Dynamite M1	Quarry and rock cuts		6,100 mps 20,000 fps	0.92	Dangerous	Good
Straight Dynamite (commercial)	Land clearing, cratering quarrying, and general use in rear areas	No. 6 commercial cap	40% 15,000 fps	0.65	Dangerous	Good (if fired within 24 hours)
50%			18,000 fps	0.79		
60%			5,800 mps 19,000 fps	0.88		
Ammonia Dynamite (commercial)	Land clearing, cratering quarrying, and general use in rear areas	No. 6 commercial cap	40% 2,700 mps	0.41	Dangerous	Poor
50%			3,900 fps 3,400 mps	0.46		
60%			11,000 fps 3,700 mps	0.53		
Gelatin Dynamite (commercial)	Land clearing, cratering quarrying, and general use in rear areas	No. 6 commercial cap	40% 2,400 mps	0.42	Slight	Good
50%			7,900 fps 2,700 mps	0.47		
60%			8,900 fps 4,900 mps	0.76		
16,000 fps						

Figure 4.2: Explosive Characteristics (Source: US Army FM 5-25)

Because of the different characteristics described above, one pound of C4 is clearly not exactly equal to 1.34 pounds of TNT. However since we are interested in finding pressure at a given distance, and at these distances the pressures generated depend mostly on explosive weight and distance to target, therefore the differences are neglected. For simplicity, this paper will assume that all blasts are generated by TNT.

4.3 Pressure Calculation

As previously discussed, the detonation of an explosive creates a shockwave formed by hot, rapidly expanding gases. As the shockwave expands, the pressure and temperature dissipate until the pressure is lower than the air pressure of the surrounding area, creating a negative pressure front that is usually less severe but longer lasting. The diagram below from FEMA's Risk Mitigation Handbook shows the general shape of a shockwave from its arrival at a target through the return of the wave to normal atmospheric pressure. This pressure wave can be conservatively modeled by a triangular load with an instantaneous peak at the time of arrival and a linear decrement from the peak incident pressure to the atmospheric pressure line at the time the actual graph switches to the negative pressure phase (Baker 5).

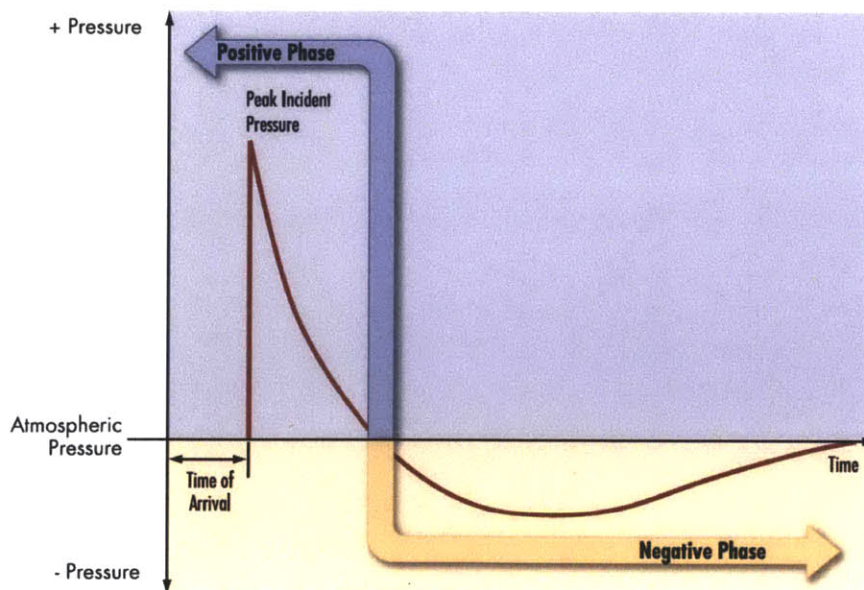


Figure 4.3: Typical Incident Pressure Graph (Source: FEMA Handbook)

In order to calculate the incident pressure on a given surface due to a shockwave, the distance from the explosive to the target surface must be scaled by the cube root of the explosive weight as shown in the equation below (Baker 54). Z is the scaled distance in $\text{lb}/\text{ft}^{1/3}$. R is the distance to the target in feet, and W is the explosive weight in equivalent pounds of TNT.

$$Z = \frac{R}{W^{1/3}}$$

The scaled distance represents the blast density. For example a change of one pound at a standoff distance of one foot would have the same blast density as a charge of 1000 pounds at a standoff distance of 10 feet. Once the scaled distance is known, several equations, such as the one below (Smith and Hetherington 33), can be used to predict the peak overpressure where Z indicates the scaled distance found above, and P_{so} indicates the peak incident overpressure in bars.

$$P_{so} = \frac{6.194}{Z} - \frac{0.326}{Z^2} + \frac{2.132}{Z^3}$$

The greatest value of under pressure was also empirically described by Brode (Smith and Hetherington 35) and is shown below.

$$P_{\min} = \frac{-0.35}{Z}$$

Since the minimum pressure is usually far less than the peak overpressure, the peak overpressure is usually the critical value when considering damage to a structure.

Using these relationships it is possible to convert the blast loads considered from table 3.1 into Z values, and then use those Z values to predict the incident blast overpressures that would result from the considered loads. A table displaying the calculated Z values and a graph showing the resultant overpressure are shown below. The graph clearly shows that decreasing Z values represent a higher

blast density, which results in a greater overpressure. Higher Z values represent a lower blast density, or greater standoff, which results in a lower overpressure.

Table 4.1: Factored Distances for considered Loads

Source	Explosive Yield, lbs TNT	Standoff Distance, feet	Factored Distance (Z)
Man Portable	5	5	2.924017738
	50	10	2.714417617
	50	20	5.428835233
Sedan	300	25	3.734503955
	300	50	7.469007911
Van	1000	40	4
	1000	160	16
Truck	5000	40	2.339214191
	5000	200	11.69607095
	10000	400	18.56635533

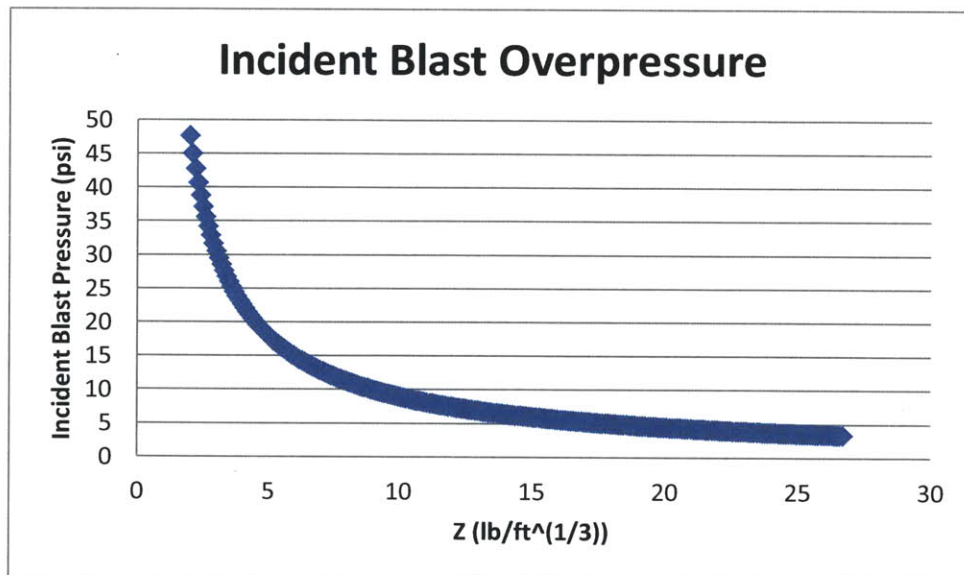


Figure 4.4: Expected Overpressures from Calculated Z Values

When the incident pressure strikes a surface such as the wall of a building, a reflected pressure wave is formed that may be much greater than the incident wave. The reflected wave is usually considered to act on the surface rather than the incident wave. In general, the closer the surface is to being orthogonal to the incident wave, the greater the magnitude of the reflected pressure wave. Tables predicting the

peak reflected pressure were published by Baker in 1973, and the figure 4.5 from FEMA's Risk Management Handbook below gives a general idea of the reflected pressure coefficients. In order to find the maximum reflected pressure for a given incident pressure, the angle is identified, and projected vertically onto the appropriate curve. Then the incident pressure is multiplied by the ordinate value to give the reflected pressure.

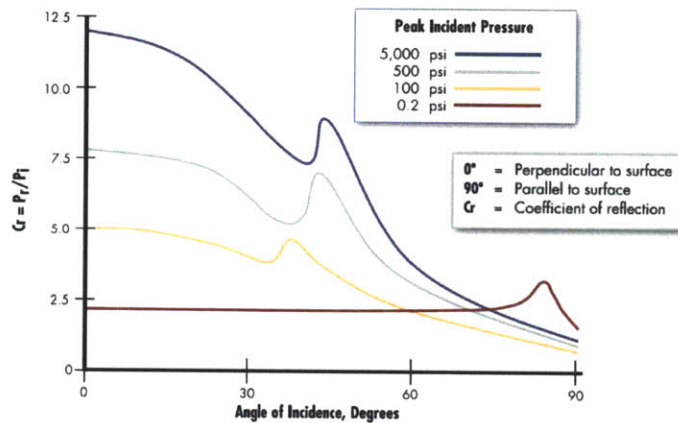


Figure 4.5: Reflected Pressure Coefficients (Source: FEMA Handbook)

As shown in the graph, in cases where the angle of incidence is perpendicular to the target surface and the incident pressure is quite large, the coefficient of reflection can be enormous. However, incident pressures with the larger magnitudes shown are highly unlikely; values between .5 and 10 psi are more reasonable values for peak incident pressures based on the considered blast loadings, based on the Z values calculated above.

Impulse, which is a measure of the energy absorbed by the structure from the explosion, is simply the integral of the incident pressure wave taken over time. A graph of a typical impulse waveform taken from the FEMA Handbook is shown below.

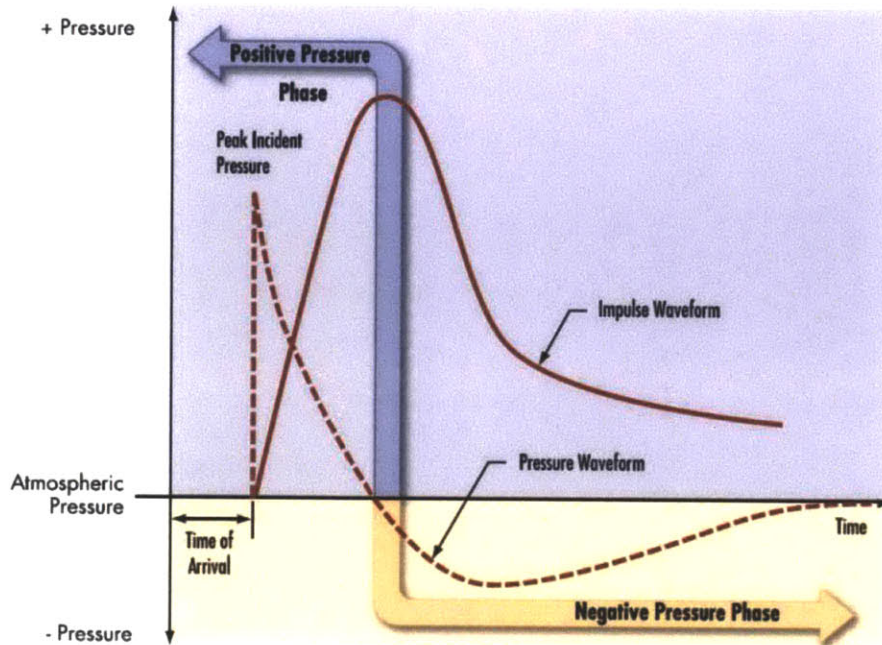


Figure 4.6: Typical Impulse Waveform (Source: FEMA Handbook)

4.4 Structural Reaction to Blast Loading

Put simply, the natural period of a structure determines whether the peak reflected pressure, the impulse waveform, or dynamic behavior governs the structure's response to the blast (Smith and Hetherington 162). The factor T_d describes the time between the incident wave's arrival and its transition to the negative pressure phase, or the time between the beginning of the impulse curve and its peak. If the structure's natural period (T) is substantially shorter than T_d , then the peak blast loading and the structure's stiffness govern the response. The loading can be considered quasi-static in this case because structure's full deflection will be reached prior to the force decreasing significantly. If the natural period is longer than T_d , the impulse loading will control the response because the structure will most likely continue to deform after the load has been absorbed. If the natural frequency of the building is similar to T_d , the building will behave dynamically and can be modeled as a single degree of freedom system reacting to a decreasing triangular load, which is a simplified version of the impulse waveform. A detailed description of the dynamic behavior of the system, along with pertinent equations, is given in

Smith and Hetherington chapter 9. The diagram below from Baylot et. al shows the general regions for which each of the mentioned loading types governs.

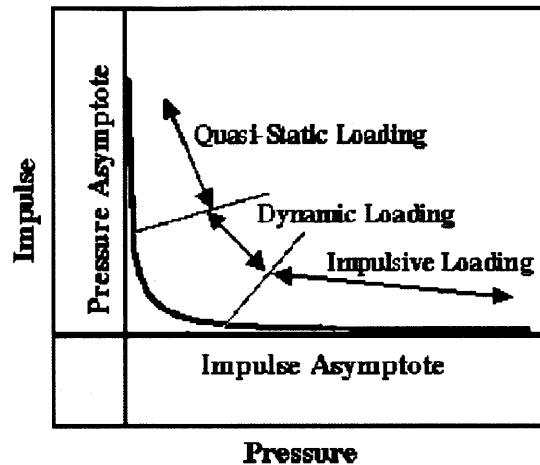


Figure 4.7: Structural Response Regions (Source: Baylot et al.)

For this paper, the Blast X program described in the following section generates a loading time history. The time histories are then imported into SAP 2000 and applied directly to the finite element models used. The model then responds to each individual time step loading. The model's reaction to the time step loadings automatically takes into account the structure's natural period, and therefore the structural response will imitate the reactions predicted above. Since blast loadings are generally timed in ms, and structural natural frequencies generally range from seconds to hundredths of seconds, most structures are governed by the impulse response under most loads. Further information regarding the SAP 2000 models of the structures considered is contained in the building model section of this paper.

4.5 Blast X

For this paper, the program Blast X will be used to determine the blast loadings that will be incident on the building models. Blast X was developed at the Engineering Research and Development Center branch of the US Army Corps of Engineers located in Vicksburg, MS. The program is significantly more advanced than is required for the purpose of this paper, and accepts various inputs which can be used to compute shock and gas venting throughout a structure with up to twenty rooms with varying

geometries. Since the primary purpose of this paper is to determine the ability of various buildings and reinforcement schemes to withstand blast loadings originating from the outside of the structure, it will only consider the effects of blasts of the sizes and distances previously discussed incident on the outside of a structure. Blast X will create time histories of incident shock wave pressures on each face of each of the hypothetical buildings.

4.5.1 Inputs

As mentioned, the Blast X program was designed to calculate blast waves for extremely specific problems, generally involving indoor explosions. Therefore the program is able to be customized extensively so that it is tailored to meet the conditions for almost any situation. For example, ambient temperature and pressure conditions, wall thermal coefficients, and amount of oxygen present can all be customized. For the purposes of this paper, these variables will all be set to their default values. The inputs of primary importance to this paper are the room geometries, explosive characteristics, and target locations.

Blast X was designed to primarily be used with interior explosions, so the best way to model an exterior explosion is to model the building geometry in question, and then place a much larger room next to the model geometry, which represents the exterior (Britt et al., 22). The explosive is placed inside the larger room, near the building to be modeled. The other walls of the larger room are several orders of magnitude further from the explosive. The explosive is then modeled by the program, and the building is affected by the blast waves directly. The blast waves must travel to other edges of the larger room, and do not have sufficient magnitude to affect the building when they are reflected and return.

Blast X also allows the explosives modeled to be extensively customized. The explosive material, shape, charge weight, and charge casing are all adjustable. Multiple charges with different times of explosion, and charges with multiple different explosive components are also modeled. For the purposes of this

paper, a simple spherical TNT explosive with the charge weights and distances discussed above are used as inputs.

In order for Blast X to determine temperature or shock wave time histories, the user must also input target locations. The program then executes the explosion simulation and calculates the time histories of shock waves incident on each designated target.

Figure 4-8 below is a simple example of several views of a single room showing a charge located in the center of the room and target located along one wall. If this simulation were run, the program would record the shock wave time history at the target point due to an explosion of designated size in the center of the room.

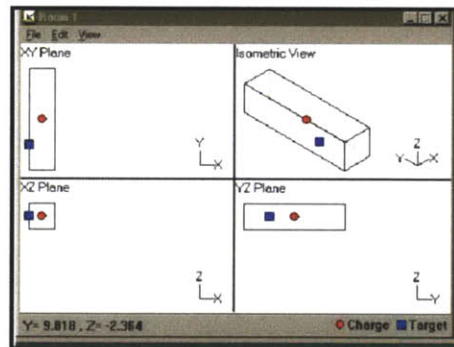


Figure 4.8: Example Blast X Input (Source: Blast X User's Manual)

The final input considered is the input "maxord" which simply describes the number of times blast waves should be considered to reflect off of walls inside a building. Since loading densities considered are relatively high, the programmers recommend the use of a maxord of 2 which is followed for this paper (Britt et al, 6).

4.5.2 Calculations

Depending on the explosion being modeled, Blast X calculates the values of explosive in one of two ways. For simple calculations, tabular data on pressure, particle velocity, and density waveforms

calculated using the RAGE Hydrocode are included in the program (Britt et al., A1). The tables contain all the necessary significant data for simple spherical TNT explosions at scaled distances out to 18 lb/ft^{1/3}, which is sufficient for the purposes of this paper. The program simply interpolates the table data to provide time histories of incident blast pressures on requested targets. For explosions that do not have tabular data included in the program, Blast X uses one of two equations shown below to calculate the requested time histories (Britt et al., A5).

$$P(t) = P_{so} [1 - (t - t_A) / t_0] e^{-(t-t_A)/\theta_+} \quad \text{for } t \leq t_A + t_0$$

$$P(t) = -G e^{-(t-t_A-t_0)/\theta_-} \sin [(t-t_A-t_0)/\phi] \quad \text{for } t > t_A + t_0$$

The graph below represents a typical waveform generated by the equations above.

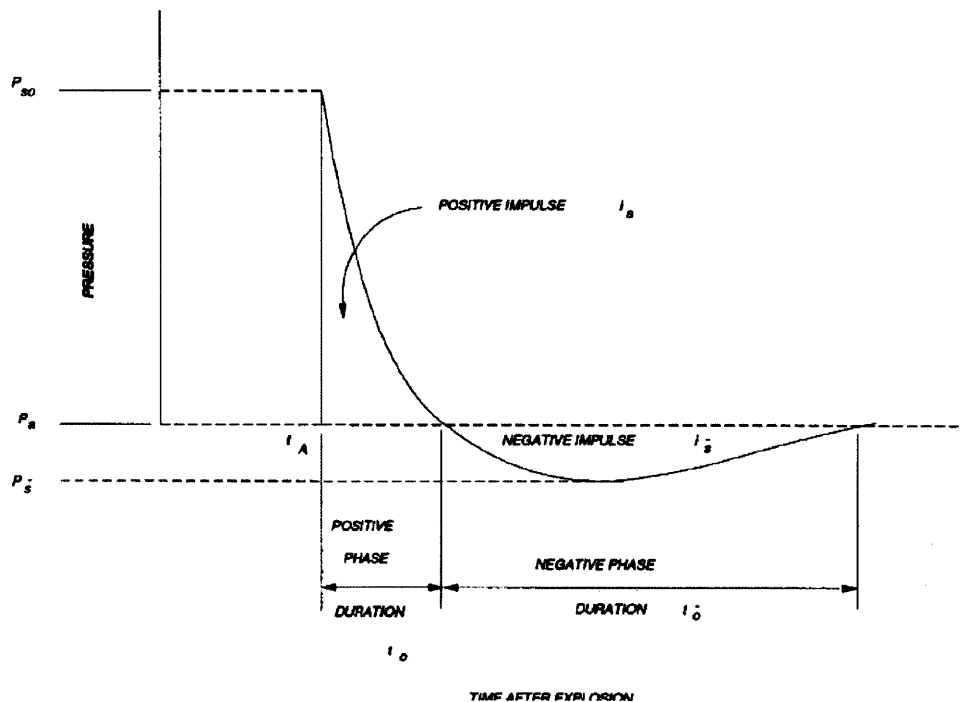


Figure 4.9: Example Calculated Pressure Waveform (Source Blast X User's Manual)

The tabulated data are more accurate than the equations used to generate data, and are recommended for use by Britt et al. For simplicity and accuracy, this paper will only consider a spherical blast for which there are tabulated data; therefore further discussion of the equations and their parameters is omitted here. Detailed descriptions of the variables are available in the Blast X user's manual. As a final note,

Blast X can also calculate wall failures, but because the interface in SAP 2000 is more easily set up and altered, and the data are easily exported from Blast X and imported into SAP 2000, this paper will use SAP 2000 finite element models to predict wall failure.

4.5.3 Outputs

As a validation of the accuracy of the Blast X models, the programming team ran a program of tests wherein they gathered data from an explosion's effect on a series of rooms, and tested against the code. A typical result taken from the Blast X user's manual is shown below (Britt et al., 38).

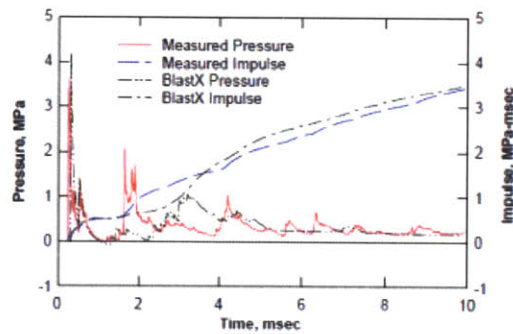


Figure 4.10: Blast X Validation graph (Source: Blast X User's Manual)

Based on these results, Blast X is considered to be an appropriate tool to model an explosion's effect on a simple structure. Targets will be placed as shown in figure 4.11 and a pressure time history will be generated for each one, which will then be exported to be applied to the SAP 2000 model. The figure on the left shows the relationship between the large room that models the exterior on the left, and the smaller room modeling the building on the right. The red dot denotes the placement of the charge in the first room which models the exterior, and the two blue dots denote the targets on the outside face of the building. Room 2 is shown in small scale in the right half of the left figure, and in larger scale in the right figure to more clearly show target placement inside the building.

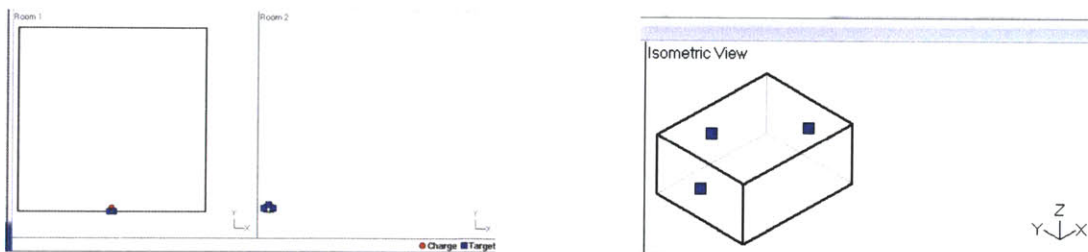


Figure 4.11: Blast X Input Examples

5 Building Models

The next step after determining the threat and modeling blast effects was to model the building resisting the blast. The finite element modeling program SAP 2000 was used to create the models and determine the effects of the blasts. Three models were used for the purposes of this paper, each made of cast in place concrete. The first model assumes that the building has doors and windows that do not resist the blast loading. The second model assumes that the windows effectively resist the blast as concrete does. The third model makes the additional assumption that a door with sufficient strength to withstand the blast is present and closed against the blast, effectively making the wall a complete concrete face. The assumptions regarding the doors and windows are reasonable, as many concrete structures present in austere environments have relatively thick steel doors, and many windows are filled with sand bags that can absorb significant blast energy through deformation. Earthen, adobe, and concrete masonry unit construction are also quite common in austere environments. However in order to make accurate comparisons between a series of models with different assumptions, concrete was chosen as a representative material. The geometry of each building was the same to allow comparisons in failures. Each building is modeled as 25 feet wide, 20 feet long and 12 feet high, with the blast being incident on the 25 foot wide face. The buildings will each be modeled using 2000 and 4000 psi concrete, with 4000 psi concrete indicating the performance of a typical building made with standard concrete, and the 2000 psi concrete being used to model weak or extremely weathered concrete. The 2000 psi concrete is considered because concrete in austere environments is often old, weathered, and constructed using aggregate material that does not belong in concrete, such as cardboard, trash, or Styrofoam.

5.1 Building Model with Door and Windows

The initial model considered will be modeled as having a door that is 5 feet wide and 8 feet tall that allows the blast pressure freely into the building. Two windows will be modeled on each side of the door, with three windows on the rear 25 foot face. Three windows will be modeled on each 20 foot face. Each window will be 2 feet wide and 5 feet tall, located at a height of 3 feet off of the ground. The building will be modeled as being constructed all in one pour, with each of the walls fixed to each other and the roof. The walls will be modeled as pinned to the ground every foot in order to prevent unrealistic stress concentrations that may affect the behavior of the model. A picture of the SAP 2000 model is shown below.

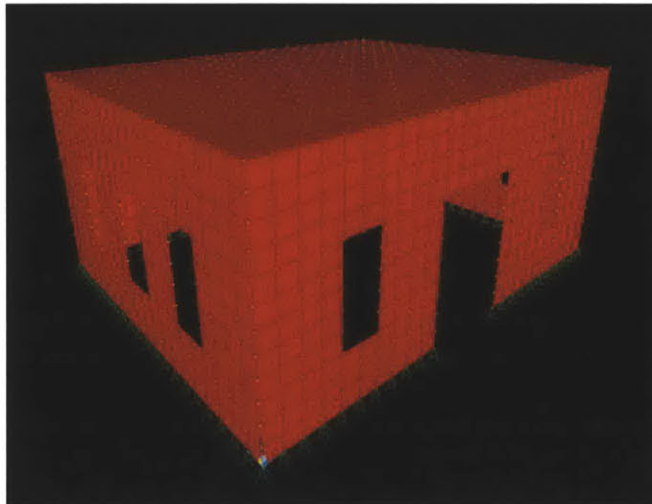


Figure 5.1: SAP 2000 Model with Door and windows

5.2 Building Model with Door Only

The second model will be considered as having a door similar to the first model. Each of the windows from the previous model will be considered to have been boarded over using a scheme that evenly transmits the load absorbed to the concrete around it. This allows the windows to be simply modeled as continuous with the surrounding concrete. The remainder of the building's features will be modeled identically to the previous model. A picture of the SAP 2000 model is shown below.

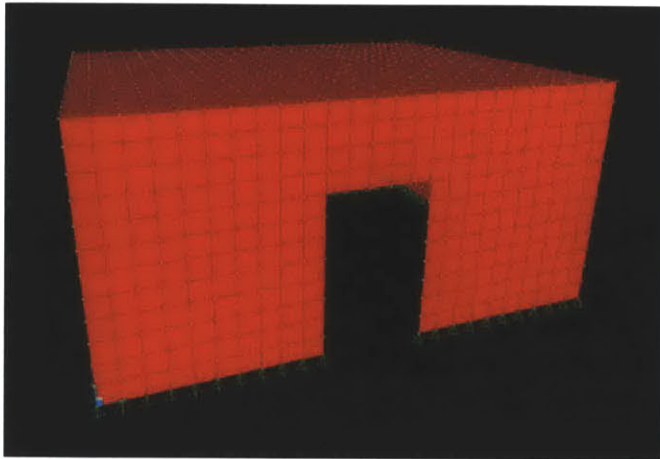


Figure 5.2: SAP 2000 Model with Door only

5.3 Building Model with no Doors or Windows

The third model will be the same as the second, with the exception that a door is present, sufficiently strong, and closed against the blast. Therefore the structure is modeled as a concrete cube. A screen shot of the wire model of the structure is shown below.

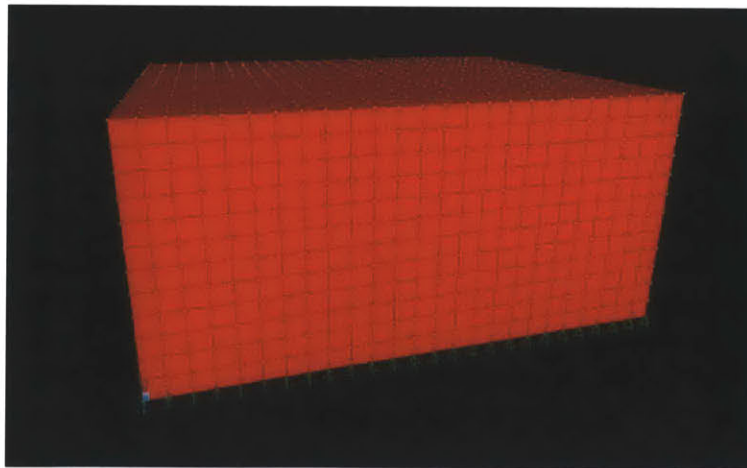


Figure 5.3: SAP 2000 Model With No Doors or Windows

5.4 Model Failure Criteria

The blast loadings will be assumed to cause wall failure either in flexure or shear. Since it is unrealistic to assume to know the layout and capacity of the reinforcing steel contained in the concrete, exact failure criteria are difficult to establish, and therefore certain assumptions will be made. The allowable shear stress of the concrete will be assumed to be equal to twice the square root of the compressive strength of the concrete, with a .85 reduction factor.

The allowable applied moment will be assumed to be determined by the modulus of rupture, which will be assumed to be 7.5 times the square root of the compressive strength of the concrete. The critical moment will be assumed to be the modulus of rupture times the gross moment of inertia of the wall section, divided by the distance from the center of the concrete section to the edge of the concrete section.

Some cracking, spalling, and other damage is expected in almost any explosion, however if either of the values determined using the methods above are exceeded on average across a significant portion of the building, it will be considered to have failed.

5.5 Model Limitations

Clearly existing concrete structures found in operational environments should not be assumed to be designed according to American building codes. In order to account for this, each building model will be tested twice, once with 4000 psi concrete, and once with 2000 psi concrete. These are clearly not the only two possibilities, and a building would need to be tested in order to determine the strength of its concrete before using the method described in this paper. In addition, doors and windows acting perfectly as part of the concrete structure is also unlikely, however the assumption is made because the effects of the doors and windows cannot be known without choosing an actual structure to model.

6 Initial Simulations

Prior to actually conducting the simulations, a separate initial simulation was conducted to ensure the accuracy of the Blast X and SAP modeling process. After the process was determined to be accurate for a loading on one wall, the simulation was run for a concrete building without any further reinforcement.

6.1 Calibration Simulation

Because limited literature exists stating the accuracy of the method to be used, a calibration simulation was run in order to ensure that the modeling method would produce appropriate results. Information on concrete blast testing was taken from the full scale blast tests on unprotected concrete conducted by Schenker et al. and replicated through the simulation method described in this paper. Schenker et al. conducted a blast test on concrete panels using a 1000 kg TNT charge with a 20 meter standoff, which gives a scaled distance of approximately $2 \text{ lb/ft}^{1/3}$ using the methods described above. This loading density is slightly greater than the worst loading case considered in this paper. The tests were conducted using a bare concrete panel and a panel covered in aluminum foam. The panels were secured side by side in the manner shown below in a support developed by “Wolfman Industries (Schenker et al., 186).”

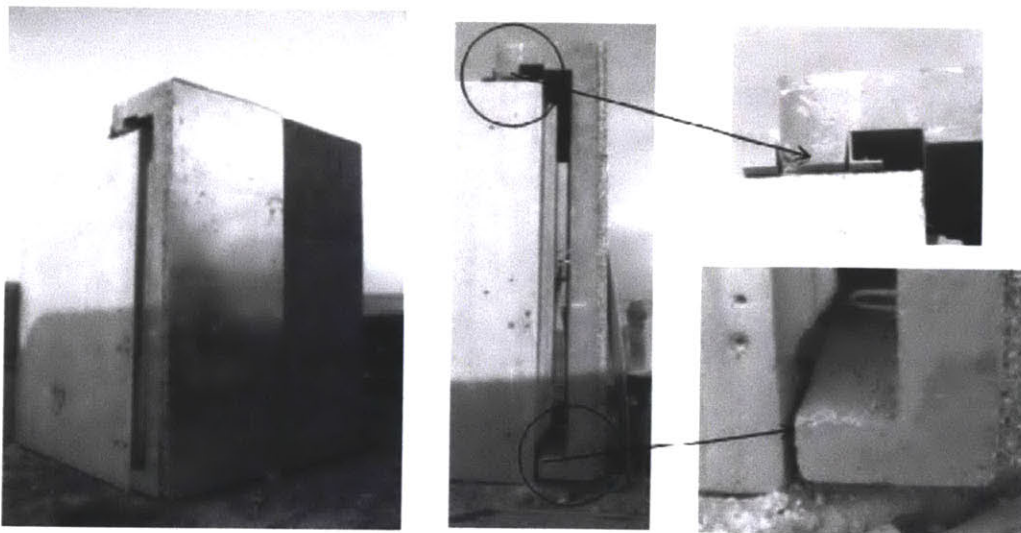


Figure 6.1: Concrete Blast Test Setup (Source: Schenker et al.)

In order to model this system, the panels will be assumed to be pinned along the top and bottom. The height of each panel is given as 3m, and the width and thickness are assumed to be 1 m and 8 cm respectively, based on the pictures. Other properties of the concrete are explicitly stated and can be entered directly as inputs into the SAP 2000 model. The model is shown below.



Figure 6.2: SAP 2000 Concrete Panel Model

Blast X was used to model the blast waveform measured by Schenker et al. The measured waveform is shown below. The Blast X model does not contain the secondary spike shown below because that spike was caused by a reflection from a nearby surface that was not part of the experiment (Schenker et al. 190).

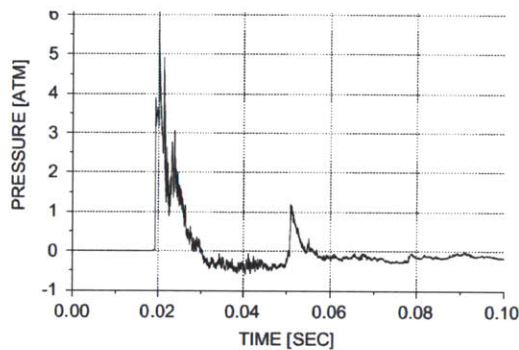


Figure 6.3: Incident Pressure Waveform (Source: Schenker et al).

The results of the blast on a concrete panel are thoroughly documented by Schenker et. al, however for the purpose of determining the accuracy of the model, the value reported for the maximum displacement of the center of the slab will be used. To measure this value, Schenker et. al used a

deformable “comb” with each bent tooth indicating about 2mm of displacement. The deformed comb members indicating about 44mm of displacement is shown below.

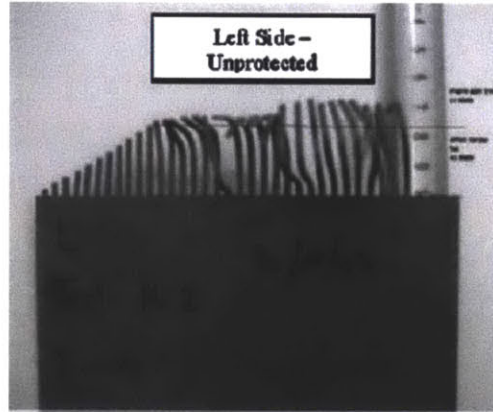


Figure 6.4: Blast Deflection Measurement Device (Source: Schenker et al.)

The pressure time history generated by Blast X was applied to the SAP 2000 model. The model is then analyzed using a non-linear modal history analysis to determine the maximum stresses and displacements resulting from the blast wave. The displacement of the SAP model under the pressure wave generated by Blast X was 42 mm, which is an error of about 2% and is about as much accuracy as can be expected when modeling blast waveforms. The deformed profiles in the SAP 2000 model and in the actual concrete match closely and are shown below.

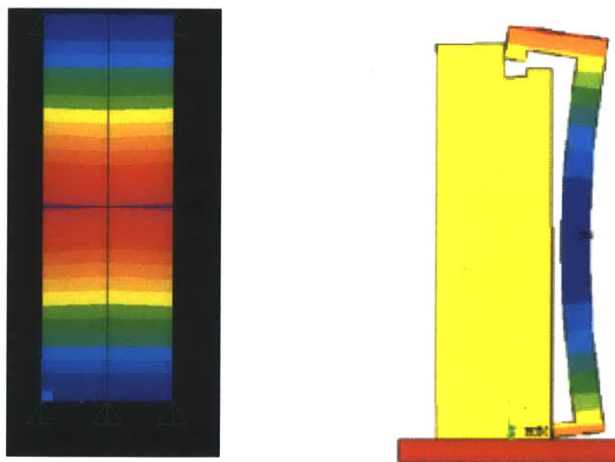


Figure 6.5: Comparison of Deflected Shapes (Source: SAP 2000 output and Schenker et al.)

As a basis for comparison, the waveform was also modeled as a triangular time history in SAP and a deflection of 46 mm was calculated, which also represents an error of about 2%. This increase in error is probably attributable to the extra energy assumed to be added to the system by the triangular model.

Based on the results of the simulation, it was determined that the Blast X and SAP 2000 modeling process would produce relatively accurate results, and that modeling blast forms with triangular approximations would produce accurate but slightly conservative results.

6.2 Unreinforced Simulation Results

After determining that the method in question was realistic, each building model was subjected to blast loadings from the threats determined above.

6.2.1 Model with no Door or Windows

The first model tested was the completely closed model with no doors or windows. The results for this simulation were likely to be the most comparable to the testing conducted by Schenker et al. and were therefore initially used to determine the accuracy of the simulation. The largest loading in the simulation was a scaled distance of $2.33 \text{ lb/ft}^{1/3}$ compared to a Z value of 2 for the experiment above. As an initial comparison, a deflection of .76 inches (19 mm) in the center of the slab was compared to the value of 43 mm observed above. Because the sample above was thinner, 8 cm as compared to 15 cm for the building model, the smaller deflection in the building was expected. An additional simulation with the same building geometry but with the wall thickness reduced to 8 cm was run to ensure that the results were reasonable. The second simulation returned a deflection value of about 90 cm. When accounting for the differences in loadings, geometry, and concrete material between the simulation and the tests run above, the increased deflection seems reasonable. The deflected shape of the building modeled in 4000 psi concrete with no doors or windows is shown below.

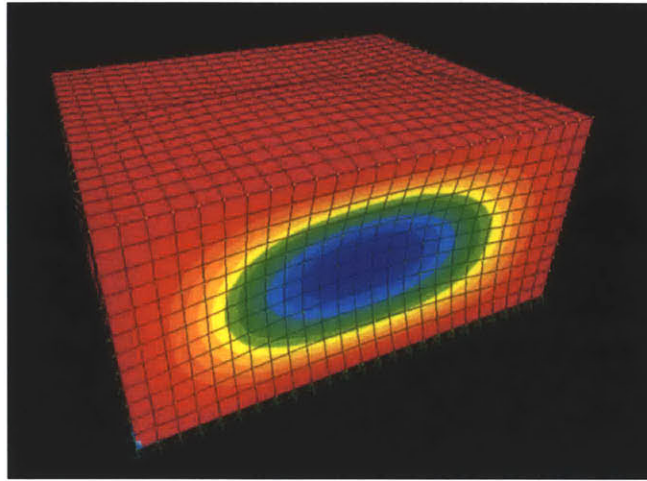


Figure 6.6: Deflected Shape of Building without Door or Windows

As expected, the base of the building did not move, but the roof is moved backward from the blast, and the side walls are leaned back and slightly bowed out. The rear wall is leaned backward from the rearward lean of the side walls and rearward translation of the roof. The most prominent feature is obviously the center of the front wall which is deformed inward significantly. The deflected shape of the model is similar under all of the blast loadings; the larger blasts simply magnify the effect. The shape is also constant between the 2000 and 4000 psi concretes. The magnitude of deflection is greater in the case of the lower strength concrete because it experiences more inelastic deformation.

The flexural loadings are also as expected for this model. The maximum flexural loading is always in the center of the front wall, while the magnitude varies with the factored size of the blast load, as would be expected. Since the base of the building is modeled as pinned to the ground, it can take no flexural load. However the flexural loading is transferred to the roof since that connection is fixed. The maximum loading for the $z = 2.33$ case is approximately 354 kip feet, which is far too large to be resisted by a relatively thin concrete wall. The flexural loading decreases as it reaches the side walls, but the wall remains overloaded across approximately 95% of its width which would almost certainly lead to failure. The flexural load pattern is shown below.

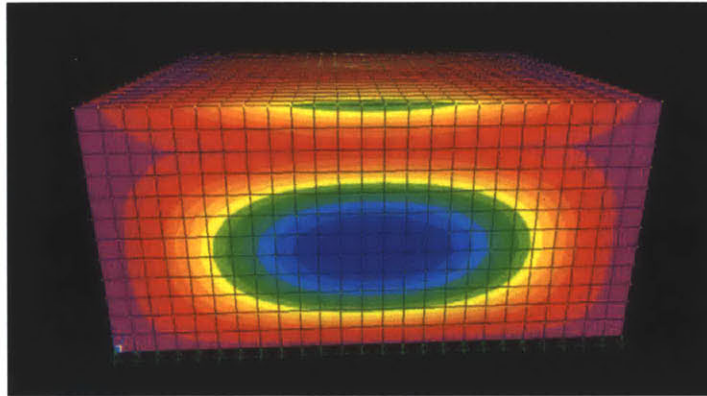


Figure 6.7: Flexural Loading of Building without Door or Windows

In addition to the flexural loadings, the building is also susceptible to failure under shear loadings. The building experiences stress concentrations at the lower front corners that far exceed its shear capacity. The shear loading distribution is shown below. Again, each of the building cases experience the same general loading pattern, the magnitude simply varies with the magnitude of the blast loading.

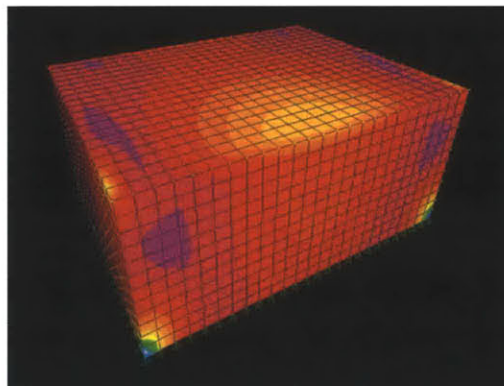


Figure 6.8: Shear Loading of Building without Door or Windows

Overall, the largest (smallest Z) loading that the 4000 psi building can take without failure is the Z of 11.69 $\text{lb}/\text{ft}^{1/3}$. The resulting moment in this case would probably still lead to severe cracking across the middle one third of the building's face, but the moments on each outer third are within tolerance and the building does not fail in shear. Based on the same reasoning, the 2000 psi model will fail during every blast up to a density of Z equal to 16 $\text{lb}/\text{ft}^{1/3}$.

6.2.2 Model with Door, but no Windows

The building model that includes the door but no windows performs in much the same manner as the model with no doors or windows. Since the building is open, it also allows blast waves to affect the rear and side building walls from the inside, which causes some additional deflection in the rear and side walls. However the major loadings still act on the front face of the building, and the largest deflection is concentrated around the gap representing the open door. The deflected shape is shown below.

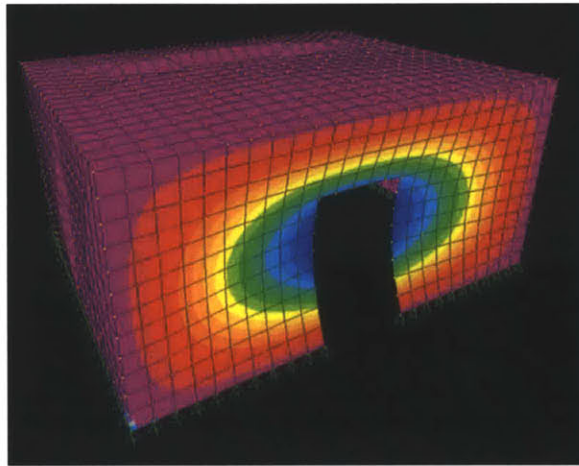


Figure 6.9: Deflected Shape of Building with Door but no Windows

The flexural loadings have concentrations at the top of the front face and near the top corners of the doorway due to the absence of the door. This behavior is supported by the experiment conducted by Mays et al., which predicts cracking patterns around openings in concrete buildings. The flexural loading pattern is shown below.

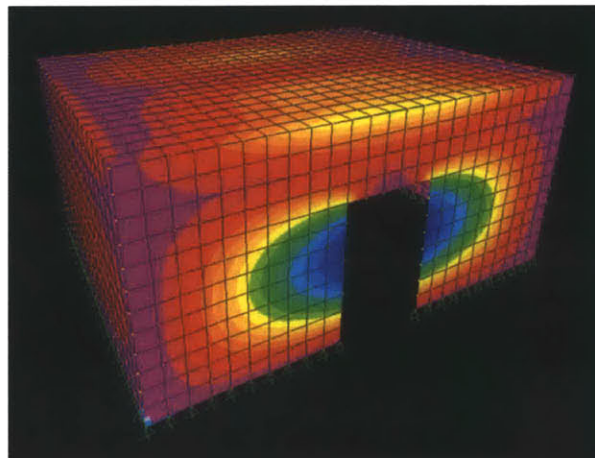


Figure 6.10: Flexural Loading of Building with Door but no Windows

The shear loading case looks similar to the case with no doors with the same stress concentrations at the front lower corners of the building. The no door case also has non-critical stress concentrations at the top corners of the door. The shear loading case is shown below.

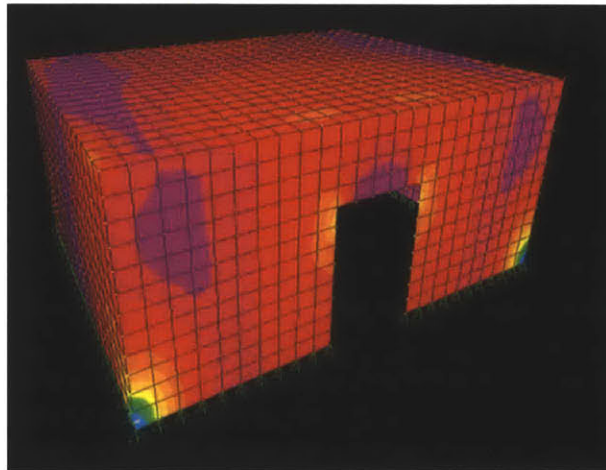


Figure 6.11: Shear Loading of Building with Door but no Windows

The overall displacement and maximum flexural loading are similar to the model with the completely closed face, but each value is slightly higher due to the removal of the front door. Both the 4000 psi model and 2000 psi model are able to withstand the same blast loading concentrations as their corresponding models without doors. Each of these models would probably fail in flexure, with cracking beginning near the doors and extending to the side walls before failure.

6.2.3 Model with Door and Windows

The deformation patterns in the models with doors and windows are as expected, with the largest deformations occurring between the doors and windows. The side walls also deform slightly because they bulge outward due to the pressure on the interior of the building while being pushed into a backward lean by the pressure from the front building face. Front and side views of the deformation are shown below. The magnitude of the displacement of the building front is much larger than the side deformation; however the side deformation could cause concrete cracking in extreme loading cases. The

deflection magnitudes are similar to the case with no door or windows, and marginally smaller than the case with a door but no windows.

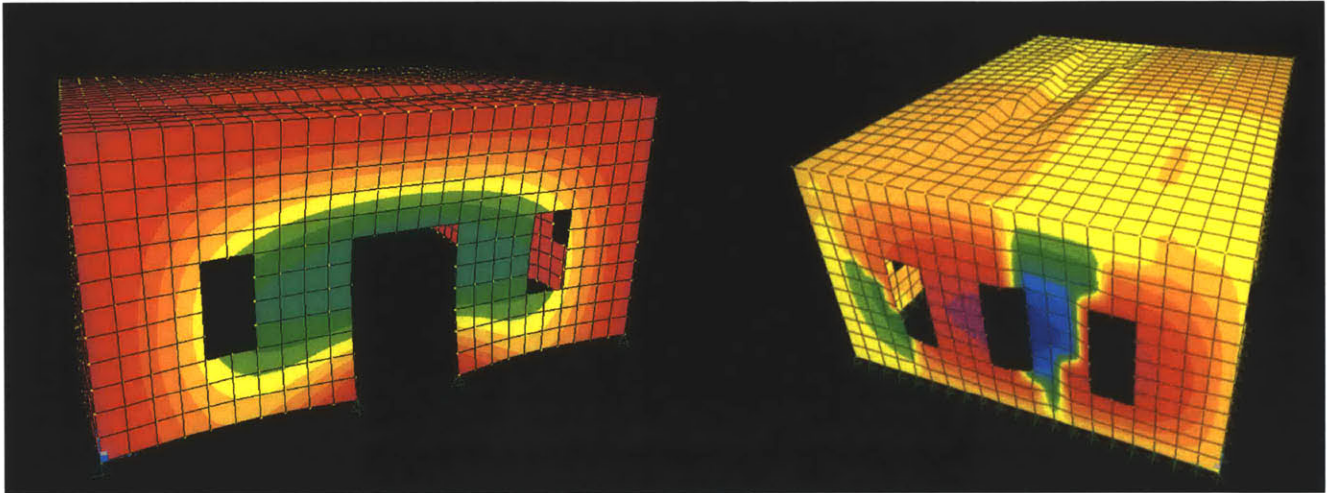


Figure 6.12: Deflected Shape of Building with Door and Windows

The flexural loadings have concentrations between the door and windows on each side, as would be expected from the deflection diagram shown. Minor concentrations are also present at the corners of the windows, but are not critical. The overall flexural loadings are lower than the previous two cases, with significant cracking limited to the area between the doors and windows. The flexural loading on the front face of the building is shown below.

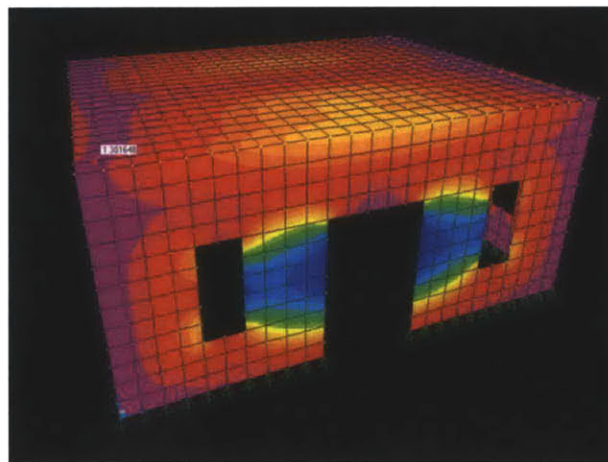


Figure 6.13: Flexural Loading of Building with Door and Windows

The shear loading in the case with doors and windows becomes much more critical. The same loading concentrations exist at the lower front corners of the building, and the same minor stress concentrations at the corners of the windows and doors exist as would be predicted from the previous cases. However larger, more critical stress concentrations also exist at the windows on the side walls. The concentrations control the strength of the models with windows and doors because of the much smaller shear area along the side walls

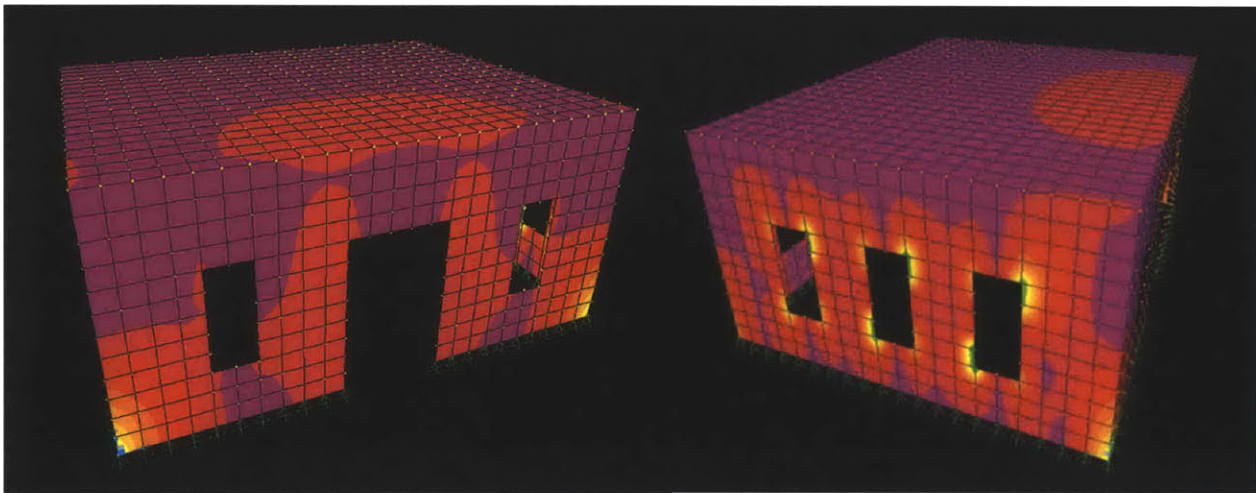


Figure 6.14: Shear Loading of Building with Door and Windows

Although the models with doors and windows experience similar deflections and smaller flexural loads than the previous cases, they come closer to failing in shear because of the decreased shear area available on the side walls.

6.2.4 Model Failure Comparison

Each of the buildings modeled with 4000 psi concrete failed under a loading density of $11.69 \text{ lb/ft}^{1/3}$. The buildings would experience significant cracking but would remain uncracked across about 50% of their front face. The model with doors and windows would also experience significant shear cracking along the lateral windows. The 2000 psi buildings would fail under loading densities higher than $16 \text{ lb/ft}^{1/3}$, and would fail in approximately the same manner as the 4000 psi buildings.

In general, the 4000 psi building models generally had lower deflections and higher resultant moments than the 2000 psi buildings because of their increased stiffness. The 2000 psi buildings had slightly lower moments than the 4000 psi buildings, but due to their much lower flexural strength they failed more easily.

In terms of the risk assessment conducted above, the 4000 psi buildings could withstand only three of the possible loadings, while the 2000 psi buildings would fail under all but two of the loadings. The buildings with openings performed nearly as well as the building modeled as a closed face, however covering the openings in the building would probably still be worthwhile in order to shield occupants and any sensitive equipment inside from blast overpressure.

7 Carbon Fiber Reinforced Polymer

Since the normally reinforced concrete buildings fared relatively poorly under blast loadings, several options were considered as reinforcement to the concrete to improve its blast resistance.

When considering options for increasing the durability of concrete in an austere environment, several criteria were considered. First, the reinforcement option had to be somewhat widely available and easily transportable. The reinforcement option also had to be applicable in all weather conditions and to any type of structural material. Finally the reinforcement had to be able to be applied to a surface quickly and by personnel without extensive training.

Carbon Fiber Reinforced Polymer (CFRP) meets all of the above criteria. It is widely available, flexible, light, easily transportable, and can be added to concrete structures by bonding it directly to the concrete using epoxy as in the testing done by Razaqpur et al., or through other methods used in testing done by Urgessa and Maji, and by Muszynski and Purcell. An additional benefit to the addition of CFRP to a concrete structure is that it will reduce the spalling of the concrete associated with the blast loading. Since the CFRP is applied in sheets and across the entire concrete slab, the CFRP panel will keep the concrete from breaking apart and acting as damaging projectiles. One drawback associated with the addition of CFRP to a concrete structure is that it can increase the structure's strength, but also may reduce its ductility (Razaqpur et al.,1367). This ductility reduction will result in higher loadings, but the additional strength will generally more than compensate for this effect.

8 Reinforced Simulations

Since CFRP is generally much stiffer in tension than in compression it was modeled as a tendon element in SAP with strength in tension but not in compression, which made the model conservative. Both faces will be considered to be coated with 2x .11mm layers of CFRP following the experiment conducted by Razaqpur et al. The additional strength in tension will increase the flexure capacity of the concrete. However, the CFRP will be assumed to add no additional shear strength, which is also conservative. The concrete reinforced with CFRP will be assumed to fail under the same conditions as in the initial test.

8.1 Reinforcement Calibration Simulations

As in the above case, limited literature exists on the accuracy of the method to be used to simulate the blast loading of CFRP concrete. Therefore a simulation of the work done by Razaqpur et al. was attempted. Razaqpur et al. conducted blast loading simulations of identical 1m x 1m x 70cm thick concrete panels, four panels with 2x .11mm layers of CFRP reinforcement on each side and four panels with no reinforcement. Figure 8.1 below shows a panel with CFRP reinforcement and one without. Note that the reinforcement is not present on the edges.

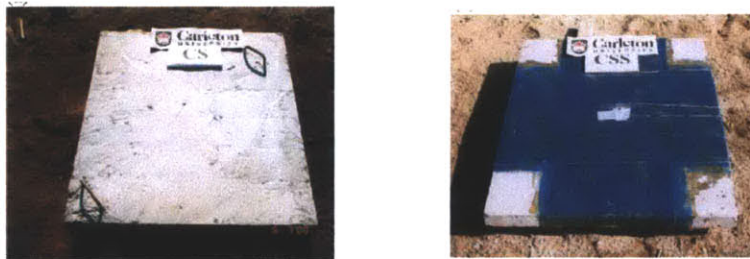


Figure 8.1: CFRP Test Setup (Source: Razaqpur et al.)

In order to model the CFRP reinforced slabs in SAP 2000, a layered shell element was created with a 70 mm concrete center and two layers of .11mm CFRP with material properties as specified in the Razaqpur et al. experiment. This model is imperfect in several ways. First, it assumes the entire face of the

concrete is covered in CFRP, which was not the case. However since the majority of the deflection happened at the center of the slab, it is a close approximation. The model also assumes that the CFRP has no compressive strength, the epoxy that bonds the CFRP to the concrete has no strength, and that the CFRP will not become de-bonded from the concrete.

For the test, the panels were placed into a holding device that was level with the ground in order to eliminate wrap around pressure. The device reduced the effected span length of the concrete slabs to 90cm per side. The setup of the test and the SAP 2000 model used to simulate the test are shown below in figure 8.2.

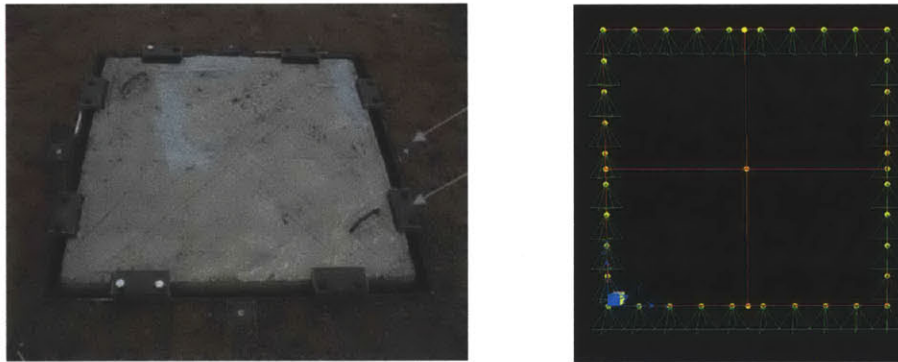


Figure 8.2: CFRP Test Simulation Model (Source: Razaqpur et al., SAP 2000)

The explosive device used in the actual test was of an irregular shape and composition and the low Z value may have been too small to allow the development of a smooth wave front (Razaqpur et al., 1376). Therefore the blast would be difficult to accurately model. However, detailed records of overpressure and impulse incident on each slab were kept. Because the method of approximately representing the blast wave with a triangular pulse was found to be relatively accurate, this method was used to approximate the blast wave generated in this case rather than data generated by Blast X.

The SAP 2000 simulation returned results that were representative of the results recorded by Razaqpur et al. for the normally reinforced slabs. However, the data collected during the experiment showed no significant reduction in deformation based on the application of CFRP, while the SAP 2000 simulation shows a deformation reduction of about 33%. Razaqpur et al. address this by saying non-uniform pressures were possible based on the irregularity and close proximity of their explosive device, and in some cases the CFRP de-bonded from the concrete. Similar experiments conducted by Muszynski and Purcell showed deflection decreases of 33% to 50% and another by Wu et al. showed decreases of up to 66%. Each of the studies used different set ups and reinforcement schemes, so the results should be expected to vary. However, based on these results and the author's statements the results from the SAP 2000 model seem reasonable and conservative. The deflected profiles of approximately 6.5 cm and 10 cm for the reinforced (left) and unreinforced slabs (right) respectively are shown below in figure 8.3.

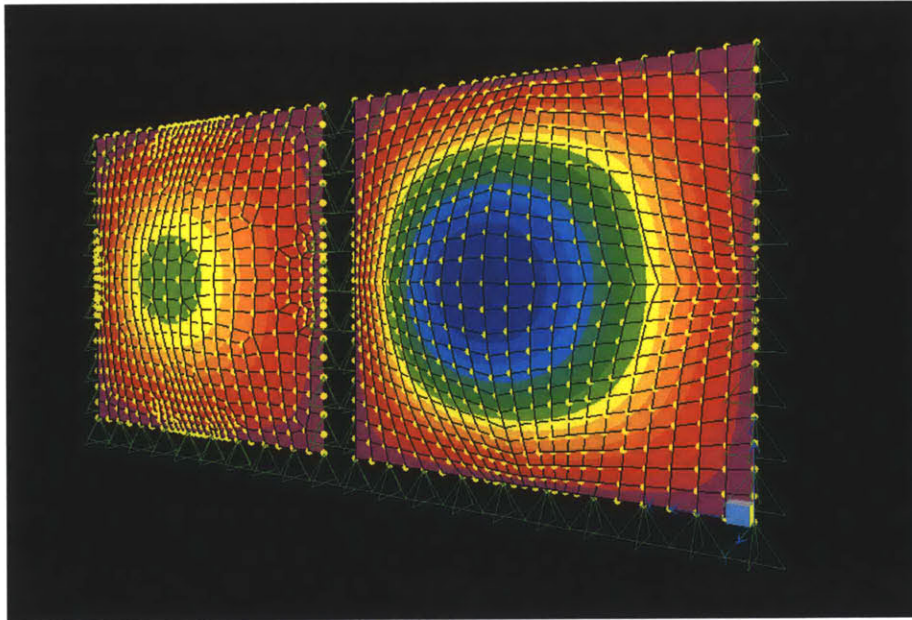


Figure 8.3: CFRP Test Simulation Deflected Profiles

8.2 Reinforced Building Simulations

After verifying the accuracy of the CFRP reinforcement model, the buildings each simulation was executed with the CFRP added to the concrete to determine the differences in loadings and deflections.

8.2.1 Building with no Openings

After the CFRP was added to the building, the deflection and flexural and shear loading patterns associated with the various loadings was the same as in the unreinforced case. However, the building was stiffer, and therefore experienced less deflection and slightly greater flexural loadings. Overall the greatest difference was in the ability of the model to accept flexural loadings. The reinforced 4000 psi building was able to absorb extremely large flexural loadings, and failed due to concentrations of shear loading at the lower front corners of the building at a blast density of $5.42 \text{ lb/ft}^{1/3}$. The 2000 psi building also failed under the shear load at a loading of $7.46 \text{ lb/ft}^{1/3}$. Since the deflection and loading patterns are the same as in the unreinforced cases, the diagrams for the reinforced cases are omitted.

8.2.2 Building with Door, but no Windows

Like the previous case, the loading and deflection patterns were similar. The deflections were smaller and the flexural and shear loads were slightly higher. The 4000 and 2000 psi buildings failed under the same loadings and for the same reasons as the buildings in the previous case. This behavior was expected due to the similarity between the building types in the unreinforced case.

8.2.3 Building with Door and Windows

The building model with a door and windows displayed slightly different behavior than the models discussed above. Like the previous cases, the reinforced models were stiffer than the unreinforced models and therefore experienced smaller deflections and slightly greater loads. However, since the models with doors and windows experience large shear concentrations at the windows on the side walls, they are more susceptible to shear failure. Since the flexural capacities of the reinforced

structures are much higher and the shear capacities are the same, the buildings with doors and windows experience much smaller overall blast load capacity increases. The 4000 psi reinforced building with doors and windows did not experience an increase in capacity and the 2000 psi building increased only slightly. Both buildings failed under a blast density of about $11.69 \text{ lb/ft}^{1/3}$.

9 Results Comparison

The figure below shows a summary of the building models and material compositions simulated.

Table 9.1: Building Maximum Loading Densities

Model	Concrete Strength	Maximum Loading Density ft/lb ^(1/3)	Failure Mode
No doors or Windows	2000 psi	Z =16	Flexure, Front face
No doors or Windows	4000 psi	Z=11.69	Flexure, Front face
Door, no Windows	2000 psi	Z=16	Flexure, Front face
Door, no Windows	4000 psi	Z= 11.69	Flexure, Front face
Door and Windows	2000 psi	Z=16	Flexure, Front face and Side Shear
Door and Windows	4000 psi	Z= 11.69	Flexure, Front face and Side Shear
No doors or Windows	2000 psi w/ CFRP	Z=7.46	Front Corner Shear
No doors or Windows	4000 psi w/ CFRP	Z=5.4	Front Corner Shear
Door, no Windows	2000 psi w/ CFRP	Z=7.46	Front Corner Shear
Door, no Windows	4000 psi w/ CFRP	Z=5.4	Front Corner Shear
Door and Windows	2000 psi w/ CFRP	Z=11.69	Shear at windows
Door and Windows	4000 psi w/ CFRP	Z=11.69	Shear at windows

In general, the more solidly built buildings, those with fewer openings and stronger concrete, have higher capacities as would be expected. Also, the CFRP was clearly effective at providing flexural reinforcement to the concrete because all of the models containing CFRP failed under shear loadings rather than in flexure. The CFRP was modeled as having no compressive or shear effect on the building, which was conservative, but possibly led to overly conservative shear failures in the building models. If the CFRP was modeled to add shear capacity, the buildings with doors and windows certainly would have had a much higher blast capacity, while the other models would have possibly been able to withstand a marginally higher load concentration at their lower front corners.

After determining the allowable blast loading density, it is possible to work backwards to determine the appropriate standoff distance to be maintained for certain explosive sizes. For example, if an existing building made of 4000 psi concrete with doors and windows were occupied, the building could be expected to withstand a blast density of $11.69 \text{ lb/ft}^{1/3}$ which corresponds to a 1000 pound device exploding 117 feet from the building. If a risk assessment determined that a 1000 pound device was likely to explode within 60 feet of the building and it was impossible to create sufficient standoff, the building could be retrofitted with strong windows and doors as well as CFRP. This would possibly allow the building to withstand a blast density of $5.4 \text{ lb/ft}^{1/3}$, which corresponds to a 1000 pound device exploding 55 feet from the building. In this way, the modeling and simulation process could lead to the effective mitigation of blast hazards.

10 Conclusions

The determination and mitigation of blast loading hazards is a problem that may become more prevalent as the US moves away from high intensity conflict and toward engaging in limited combat and peacekeeping operations. As this transition occurs, the currently utilized method of protecting the force, namely occupying a large footprint ringed with concrete walls, may become less feasible from an operational and financial standpoint. The occupation of existing structures partially solves this problem, but leaves the occupant particularly vulnerable to suicide and other explosive attacks due to the relatively poor flexural capacity of concrete and other building materials commonly found in austere environments. As has been clearly shown in multiple tests, the addition of flexural reinforcement to concrete walls can make them more effective at withstanding blast loadings. Since CFRP is widely available, easily transportable, able to be applied without training, and proven to increase a structure's blast resistance, it seems to be a natural choice for utilization in these circumstances.

Further, it seems that a reasonably simple and effective method of determining a structure's ability to withstand blasts is to model a particular blast's effects and apply those effects to a finite element model of the structure in question. This method may allow commanders to accurately assess the risks posed to their buildings by particular blast loading densities, and take actions to ensure that the buildings that they occupy are able to withstand the identified threats.

In order for the results of this paper to be validated, actual blast testing would have to be conducted on a variety of structures. The modeling process would then need to be applied to models of several tested structures to determine its accuracy over multiple cases. Further, the actual properties of the materials in question would need to be known, particularly the shear capacity of the CFRP, and the shear and flexural capacities of the concrete. Since these qualities can only be generally assumed without testing the individual materials in question, the results of the simulations must be assumed to be only generally

accurate at best. However, the process used seems to be at a minimum a good starting point for developing a reliable process for mitigating blast risks in austere environments.

References

- Baker, Wilfred E. *Explosions in Air*. Austin and London: University of Texas Press, 1973. Print.
- Baylot, James T., Billy Bullcok, Thomas R. Slawson, and Stanley C. Woodson. "Blast Response of Lightly Attached Concrete Masonry Walls." *Journal of Structural Engineering* 131.8 (2005): 1186-1193. Web. 1 April 2012.
- Britt, J. Robert, Dale E. Ranta, and Charles E. Joachim. *Blast X Code, Version 4.2, User's Manual*. Washington DC: Headquarters, US Army Corps of Engineers, 2001. Electronic.
- Davidson, James S., Jeff W. Fisher, Michael I. Hammons, Jonathon R. Porter, and Robert J. Dinan. "Failure Mechanisms of Polymer-Reinforced Concrete Masonry Walls Subjected to Blast." *Journal of Structural Engineering* 131.8 (2005): 1194-1205. Web. 1 April 2012.
- Gansler, J.S. *Department of Defense Ammunition and Explosives Safety Standards*. Washington DC: Headquarters, Department of Defense, 1999. Web. 1 April 2012.
- Grant, Rebecca. "Death in the Desert" *Airforce-Magazine* 89.6 (2006): n. pag. Web. 1 April 2012.
- Hetherington J.G. and Smith P.D. *Blast and Ballistic Loading of Structures*. Oxford: Butterworth-Heinemann Ltd., 1994. Print.
- "Khobar Towers." *GlobalSecurity.org*. n.p., n.d. Web. 1 April 2012.
- "Khobar Towers Still Imagery." *Defensemagery.mil*. n.p. n.d. Web. 1 April 2012.
- King, Kim W., Johnny H. Wawclawczyk, and Cem Ozby. "Retrofit Strategies to Protect Buildings from Blast Loadings." *Canadian Journal of Civil Engineering* 36 (2009): 1345-1355. *NRC Research Press*. Web. 1 April 2012.
- Malvar, L. Javier, John E. Crawford, and Kenneth B. Morrill. "Use of Composites to Resist Blast." *Journal of Composites for Construction* 11.6 (2007): 601-610. Web. 1 April 2012.
- Ma, G.W., and Z.Q. Ye. "Analysis of Foam Claddings for Blast Alleviation." *International Journal of Impact Engineering* 34 (2007): 60-70. Web. 1 April 2012.
- Mays, G.C., J.G. Hetherington, and T.A. Rose. "Response to Blast Loading of Concrete Wall Panels with Openings." *Journal of Structural Engineering* 125.12 (1999): 1448-1450. Web. 1 April 2012.
- Moradi, Lee G., James S. Davidson, and Robert J. Dinan. "Resistance of Membrane Retrofit Concrete Masonry Walls to Lateral Pressure." *Journal of Performance of Constructed Facilities* 22.3 (2008): 131-142. Web. 1 April 2012.

- Muszynski, Larry C. and Michael R. Purcell. "Composite Reinforcement to Strengthen Existing Concrete Structures Against Air Blast." *Journal of Composites for Construction* 7.2 (2003): 93-97. Web. 1 April 2012.
- Razaqpur, A. Ghani, Ettore Contestabile, and Ahmed Tolba. "Experimental Study of the Strength and Deformations of Carbon Fibre Reinforced Polymer (CFRP) Retrofitted Reinforced Concrete Slabs Under Blast Load." *Canadian Journal of Civil Engineering* 36 (2009): 1366-1377. NRC Research Press. Web. 1 April 2012.
- Risk Management Series: Reference Manual to Mitigate Potential Terrorist Attacks Against Buildings, Chapter 4.* Washington DC: Federal Emergency Management Agency, 2003. Web. 1 April 2012.
- Schenker, Andras, Ido Anteby, Erez Gal, Yosef Kivity, Eyal Nizri, Oren Sadot, Ron Michaelis, Oran Levintant, and Gabi Ben-Do. "Full-Scale Field Tests of Concrete Slabs Subjected to Blast Loads" *International Journal of Impact Engineering* 35 (2008): 184-198. Web. 1 April 2012.
- Urgessa, Girum S, and Arup K. Maji. "Dynamic Response of Retrofitted Masonry Walls for Blast Loading." *Journal of Engineering Mechanics* 136.7 (2010): 858-864. Web. 1 April 2012.
- US Army Field Manual 5-25: Explosives and Demolitions.* Washington DC: Headquarters, Department of the Army, 1967. 83-84. Web. 1 April 2012.
- Wu, Chengquin, Liang Huang, and Deric John Oehlers. "Blast Testing of Aluminum Foam Protected Reinforced Concrete Slabs." *Journal of Performance of Constructed Facilities* 25.5 (2011): 464-474. Web. 1 April 2012.
- Wu, C., D.J. Oehlers, M. Rebstrost, J. Leach, and A.S. Whittaker. "Blast testing of ultra-high performance fibre and FRP-retrofitted concrete slabs." *Engineering Structures* 31 (2009): 2060-2069. Web. 1 April 2012.